

PACS numbers: 74.72.Bk; 74.72.Hs; 74.25.Sv; 42.55.Lt
DOI: 10.1070/QE2003v033n07ABEH002468

Enhancement of the critical current density in HTSC ceramics by laser radiation

G.N. Mikhailova, A.V. Troitskii

***Abstract*. The experimental data on the application of laser radiation to melting YBCO(123) and Bi(2223) high-temperature superconducting ceramics aimed at the improvement of their structure and an increase in the critical current density are systematised. The short-term melting of this ceramics by CO_2 laser radiation and the subsequent annealing lead to the formation of a dense fine-grained structure. As a result, the critical current density significantly increases. The best results are obtained for the Bi(2223) ceramics: the critical current density increases by a factor of 40 and 8 at $T = 20$ K and 77 K, respectively.**

Keywords: *laser technologies, CO_2 laser, melting, amorphisation, critical current density, high-temperature superconducting ceramics.*

1. Introduction

Laser technologies are currently widely used in solid-state physics and chemistry for producing new substances with unique properties. Lasers are used in technologies for manufacturing chemical products, growing single crystals, sputtering multicomponent compounds, thermally processing and doping metal surfaces, locally doping semiconductor materials, separating isotopes, initiating and conducting photochemical reactions, etc. This scope of applications is due to a great variety of the existing types of lasers and advances achieved in the understanding of the physics of the interaction of laser radiation with matter. As a tool acting on a substance, lasers have exceptional capabilities, such as tremendous heating rates, the locality of the laser action, variable conditions, etc. These factors make it possible to use lasers for synthesising materials under nonequilibrium conditions and, therefore, to obtain substances with unusual properties.

Thus, it is natural that the application of lasers in the comparatively new field of producing thin films of high-temperature superconductors (HTSCs) allowed films with a critical current density characteristic of single crystals to be obtained (e.g., [1]).

Note that laser radiation was used in the technology of superconductors for the first time in 1973 [2], and the application of a laser helped to increase the temperature of the superconducting transition in a Nb – Sn alloy.

The aim of this work is a systematisation of the experimental studies on the application of laser radiation to melting of the YBCO(123) and Bi(2223) HTSC ceramics aimed at the improvement of their structure and an increase in the critical current density. These studies were carried out at the General Physics Institute (GPI), Russian Academy of Sciences (RAS), in cooperation with researchers of the A.A. Baikov Institute of Metallurgy and Material Science and the Chemical Department of the Moscow State University and published in Refs [3 – 5]. We deal with a development of laser technologies for massive ceramic samples.

The discovery of HTSC cuprates in 1986 gave rise to great expectations of a wide use of these materials in technology. However, it was soon revealed that some fundamental properties of HTSC materials complicate their application (especially when high-current devices are designed). It is commonly agreed that HTSC cuprates represent the most complex class of substances in solid-state physics. Crystal – chemical features of these materials manifest themselves in difficulties of their synthesis and problems of their strength and stability, which must be taken into account in all types of their treatment.

Consider briefly the physicochemical properties of HTSC cuprates for an example of $YBa_2Cu_3O_{7-x}$, since their crystal structures are similar to a significant degree. The temperature of the superconducting transition for $YBa_2Cu_3O_{7-x}$ is ~ 90 K. This substance has a layered defect perovskite-like structure with oxygen vacancies. It is precisely the layered character of this compound that determines the high temperature of the superconducting transition. The superconductivity in $YBa_2Cu_3O_{7-x}$ strongly depends on the oxygen parameter x and exists only for $0 < x < 0.3$.

It turned out that, in contrast to conventional superconductors, HTSCs have a very short coherence length and a strong crystallographic anisotropy. The coherence length of HTSCs is 5 – 10 Å along the c axis and 20–35 Å in the ab plane [6], which is an order of magnitude smaller than the corresponding value for conventional HTSCs. Such a small coherence length determines a tendency of HTSCs to the formation of weak Josephson links. Their presence leads to a decrease in the transport critical current density j_c. The same result follows from the presence of incoherent boundaries between grains. This decrease is especially significant in magnetic fields.

The high crystallographic anisotropy of superconducting cuprates leads to an anisotropy of all properties of these materials, including j_c [7]. The anisotropy and small

G.N. Mikhailova, A.V. Troitskii A.M. Prokhorov General Physics Institute, Russian Academy of Sciences, ul. Vavilova 38, 119991 Moscow, Russia

Received 23 January 2003
Kvantovaya Elektronika **33** (7) 621 – 627 (2003)
Translated by A.S. Seferov

coherence length result in a situation in which it is impossible to obtain a high critical current density in structurally imperfect HTSC samples. It is precisely such properties that are inherent in the HTSC ceramics produced according to a standard sintering process. The critical current density for the best HTSC ceramic samples at $T = 77$ K is seldom higher than 1000 A cm^{-2}. At the same time, the critical current density achieved in film and single-crystal samples at 77 K is as high as 10^6 A cm^{-2}. Note that, several applications, such as levitating platforms, magnetic shields, etc., require massive superconductors.

HTSCs refer to type-II superconductors. In an external magnetic field H for $H_1 < H < H_2$, where H_1 and H_2 are the first and second critical magnetic fields, a type-II superconductor is in a mixed state, when the magnetic field partially penetrates into it in the form of Abrikosov vortices. Superconductivity disappears in the central part of a vortex, and a closed superconducting current flows over its periphery. To minimise the dissipated energy in a superconductor in a magnetic field, it is necessary to fix the vortex lattice by introducing special pinning centres, which are structural defects with a size of the order of the coherence length.

Thus, the difference of the density of the transport critical current for epitaxial-film and single-crystal HTSCs from j_c for polycrystalline and ceramic samples, which is 3–5 orders of magnitude, is associated with a disorientation of grains and the presence of incoherent boundaries and weak Josephson links.

Therefore, to improve the current-carrying and mechanical properties of HTSCs and the chemical stability of the ceramics, it is necessary to provide the material compaction, texturing, and the formation of efficient pinning centres.

Bulk HTSC samples with a high critical current density were obtained using melting technologies (see review [8] and references therein). This method was proposed in Ref. [9] for YBCO(123) and is now known as the MTG method (melt-textured growth). A ceramic workpiece obtained as a result of long sintering was used as the initial sample. After rapid heating up to $\sim 1100\,^{\circ}$C and a short-term exposure at this temperature, the sample was slowly (for ~ 600 h) cooled to room temperature (Fig. 1). The slowest cooling with a rate of $\sim 1\,^{\circ}$C h^{-1} must take place in a temperature range of 1030–900 °C. Subsequently, this method was applied to other compounds, and the maximum temperature and cooling regimes differed in various versions of this technique. Moreover, to enhance an oriented growth of grains, a temperature gradient of up to 50 °C cm^{-1} is used at the crystallisation stage of melting technologies. $YBa_2Cu_3O_{7-x}$ samples with $j_c = 7.5 \times 10^4$ A cm^{-2} in $H = 0$ and 3.7×10^4 A cm^{-2} in $H = 0.6$ T (at $T = 77$ K) were obtained by this method [10]. A further increase in j_c was attained by irradiating samples by a flow of fast neutrons in order to produce efficient pinning centres. This resulted in $j_c \simeq 10^6$ A cm^{-2} in $H = 10^{-2}$ T and 2.0×10^5 A cm^{-2} in $H = 1$ T at $T = 77K$ [11].

Thus, the j_c values attained in record HTSC ceramic samples using melting technologies and a subsequent irradiation of samples with a neutron flow are comparable with the values characteristic of epitaxial HTSC films.

However, despite significant advances in melting techniques, these methods for processing HTSC ceramics have certain limitations.

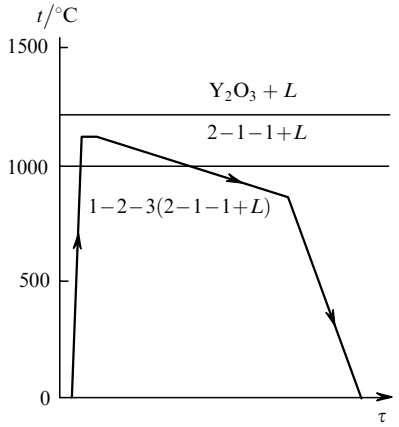

Figure 1. The regime of temperature–time thermal treatment during the production of a HTSC material of the YBCO(123) composition by the MTG method [10]. The duration of the process is ~ 600 h; L is the liquid phase; '$2-1-1$' is the Y_2BaCuO_y phase; and '$1-2-3$' is the $YBa_2Cu_3O_{7-y}$ phase.

(1) Only small samples (with a size of a few centimetres) can actually be obtained using melting technologies. (Theoretically, large samples can be obtained using the zone melting method, but the speed of the sample movement during melting is ~ 1 mm h^{-1}, which makes the obtainment of large samples impracticable). This is caused by a decrease in the mechanical strength of a sample with an increase in its length, which is a consequence of an anisotropy of thermal expansion of HTSC compounds, the localisation of impurity phases at the grain boundaries, and the appearance of stresses resulting from the tetra–ortho structural transition.

(2) The results are characterised by a low reproducibility, which is caused by the complexity of physicochemical processes forming the basis of melting technologies.

(3) The process of producing samples is very long (hundreds of hours), consumes much energy, and is conducted using expensive gradient furnaces.

Therefore, it becomes necessary to develop new highly efficient methods of processing HTSC ceramics for enhancing their current-carrying ability. One of them is the laser melting technique. Apart from lasers, IR radiation, pulsed thermal heating, and electric-current heating were also used. These methods have the following advantages: a high rate of the process; the possibility of being applied to producing long articles (wires, ribbons); the possibility of obtaining thick HTSC films on various substrates, including single crystals; the possibility of doping HTSCs in the liquid phase; and the formation of amorphous intermediate products with their subsequent crystallisation.

Let us consider some works in which these methods were used [12–14]. To increase the critical current density, pulsed laser processing of $YBa_2Cu_3O_{7-x}$ ceramics was used in Ref. [12]. The initial samples were manufactured using the standard solid-phase synthesis technology. They were shaped as rings with an outer diameter of 10 mm and different thicknesses that varied from 1.5 to 4.0 mm. The HTSC ceramic samples were irradiated by 50-ns single pulses of a 1.06-μm laser. The diameter of the laser spot was 10 mm, and the selected pulse energy density was 1.7–2.1 J cm^{-2}. The action of the laser pulse resulted in a melted layer ~ 2 μm thick, whose critical current density was much higher than j_c in the initial material. In the best sample, $j_c = 6.5 \times 10^4$ A cm^{-2} was obtained (in a thin layer). In the

initial samples, j_c did not exceed 60 A cm^{-2}. It is important that, after such processing, no subsequent annealing for restoring the super-conducting properties of the ceramics is necessary. This shows that the superconductor does not lose oxygen or this loss is insignificant.

The effect of laser processing by short pulses at a wavelength of 1.06 μm on the properties of the $Bi_{1.6}Pb_{0.4}Ca_2Sr_2Cu_3O_x$ ceramics was studied in Ref. [13]. The processing conditions were similar to those in Ref. [12]. The pulse energy density was 0.6–3.0 J cm^{-2}. Similarly to the data of Ref. [12], pulsed laser processing results in a melted layer ~ 2 μm thick with an appreciably higher j_c than in the initial material. In the melted ceramic layers, $j_c = (1.72 - 3.34) \times 10^5$ A cm^{-2} at $T = 77$ K, which is approximately three orders of magnitude higher than in the initial bulk samples. The annealing of the melted layer was unnecessary.

Two-dimensional surface superconducting structures with j_c significantly higher than j_c of the initial material were produced by laser melting on $YBa_2Cu_3O_{7-x}$ ceramics [14]. The initial ceramic samples were plates with dimensions of $50 \times 10 \times 1$ mm with $T_c = 81 - 89.5$ K and $j_c = 1$–10 A cm^{-2}. The samples placed in a hermetically sealed chamber with a controlled content of the atmosphere were processed by a continuous 1.06-μm LTI-501 laser. The diameter of the spot on the sample surface was 0.2–1 mm. The sample could be displaced normally to the direction of the laser beam at a velocity of 0.1 to 10 mm min^{-1}. A unit for controlling the radiation power stabilised the temperature at the samples' surfaces with an accuracy of no worse than ±2.5 °C. Both superconducting samples and samples transformed into a nonsuperconducting phase by baking were processed. In the first case, the irradiation was performed to improve the characteristics of samples and, in the second case, to create regions of the superconducting phase on the nonsuperconducting ceramics. The critical current density of the two-dimensional structures obtained depended on the processing conditions and amounted to $2 \times 10^3 - 2.5 \times 10^4$ A cm^{-2}. In addition to an increase in j_c, laser processing of samples stabilises the sample's characteristics, since, as a result of a compaction of the surface layer, the penetration of CO_2 and H_2O into ceramics decreases. The interaction with these substances results in a degradation of the properties of HTSC ceramics.

As was mentioned above, these studies were initiated at the GPI RAS in 1996. The effect of continuous 10.6-μm CO_2 laser radiation on $YBa_2Cu_3O_{7-x}$ and $Bi_2Sr_2Ca_2Cu_3O_y$ ceramic samples was studied. In the latter case, samples doped with finely divided Al_2O_3 and ZrO_2 powders were also used. The objective of these investigations was to select the irradiation sources and irradiation parameters: the wavelength, intensity, scanning regimes, and the conditions for the subsequent annealing for the laser methods of processing and modifying ceramic HTSCs aimed at the obtainment of a dense superconducting phase with improved current-carrying characteristics. This work included detailed studies of superconducting properties, morphology, and phase composition of samples at all of the stages of the technological process.

The optical properties of epitaxial thin HTSC films in the IR region at room temperature (reflection, absorption, complex permittivity, and complex conductivity) were studied in detail in Ref. [15]. In the normal state at room temperature, all optimally doped superconductors have metallic properties; therefore, their fundamental regularities of laser heating and cooling are similar to the behaviour of metals.

Let us analyse the case realised in our experiment. The light flux incident onto the surface of a material is partially reflected, and its remaining fraction penetrates into the body and is absorbed by it. As was shown in Ref. [15], the reflection coefficient of HTSC films of different compositions at a wavelength of 10.6 μm and room temperature lies between 0.58 and 0.9; therefore, only a part of the incident laser energy is absorbed and, due to a high absorption coefficient, it can be considered that the absorption occurs at the surface. The heated surface layer transfers the heat into the depth of the material through the heat conduction mechanism; therefore, the maximum heating temperature and the temperature distribution in the sample's depth are found from the heat conduction equation. To find more or less accurate solution to this equation, one should take into account the temperature dependences of the physical parameters of the material. Such data are absent for HTSCs, and laser-processing regimes are usually found experimentally and the heating temperature is measured with a pyrometer directly during the experiment.

2. Samples

Laser melting of HTSC samples of the $YBa_2Cu_3O_{7-x}$ and $(BiPb)_2Sr_2Ca_2Cu_3O_y$ [Bi(2223)] compositions was investigated. The initial Bi(2223) samples were synthesised by two different methods: the deposition from a solution of oxalates (at GIREDMET) and a standard ceramic technology (at the NPO Monokristall–Reaktiv). The data of an X-ray phase analysis (XPA) of the initial samples showed that the concentration of the (2223) phase in them was 93 %–95 % and 60 %–65 %, respectively.

Numerous papers point out that the superconducting properties of HTSCs improve when doping impurities, which are efficient pinning centres, are introduced into samples. We studied in detail the properties of the Bi(2223) ceramics doped with Al_2O_3 and ZrO_2 [16] and established the possibility of obtaining a sharper superconducting transition by doping samples with a small amount (1 % mass fraction) of finely dispersed Al_2O_3

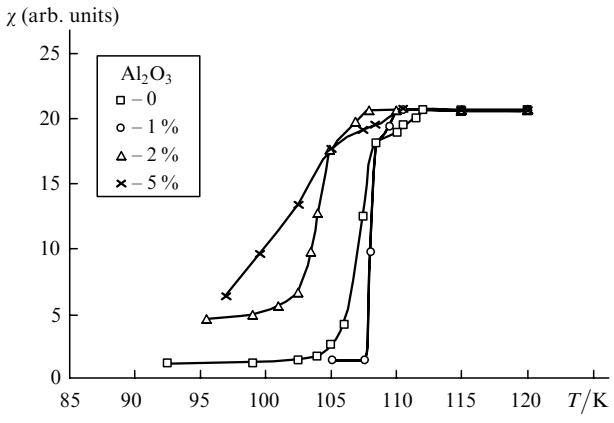

Figure 2. The effect of Al_2O_3 dopants on the shape of the superconducting transition of the Bi(2223) ceramics: (□) the initial sample; the samples in which the mass fraction of Al_2O_3 is (○) 1 %, (△) 2 %, and (×) 5 % [16]; and χ is the magnetic susceptibility.

(Fig. 2). Therefore, experiments on laser melting of doped samples were expected to be interesting. Al_2O_3 and ZrO_2 dopants (with mass fractions of 1, 2, and 5 %) were added to the Bi(2223) phase as ultrafine-grained powders (1 – 2 μm).

Ceramic samples were pressed into pellets 7 – 15 mm in diameter and ~ 1 mm thick and were then sintered for 10 h at $T = 840\,^{\circ}C$. The critical temperature T_c in the initial (undoped) material was 107 K, and the critical current density was $j_c \sim 10^3$ A cm^{-2} (at $T = 77$ K).

3. Experimental

The surfaces of HTSC ceramic samples were melted by a beam of a 10.6-μm cw CO_2 laser with a maximum power of 100 W. The beam was focused at the sample's surface into a spot with a diameter of ~ 2 mm. The beam scanning at a speed of 20 – 50 mm min^{-1} was provided by a mechanical movement of the sample. The irradiation was performed in air without an additional heater. The temperature in the zone of laser-beam focusing was monitored by an optical pyrometer. Specific conditions for laser processing were individually selected for each sample depending on the composition and state of the surface with an allowance for the phase diagram and parameters of the phase transitions. As a result of this laser action, smooth grooves 2 – 2.5 mm wide with an almost pore-free structure appeared on the samples' surfaces.

The amorphised melted layers were recrystallised by their thermal annealing in air. The temperature and duration of the annealing were selected experimentally for each superconducting material. The microstructure and the chemical and phase compositions of the samples' surfaces and their cross sections were investigated using a Jeol JSM-35 scanning electron microscope (SEM) with a LINK EDX spectrometer. The evolution of the superconducting phase exposed to annealing was studied by the XRD analysis of the melted and nonmelted sides of samples. The critical temperature and the critical-current density of HTSC were determined from measurements of the complex magnetic susceptibility.

4. Experimental results

The action of 10.6-μm laser radiation on HTSC ceramic samples leads to the partial melting of a sample and subsequent amorphisation during cooling. Investigations have shown that the amorphisation is accompanied by changes in the phase composition of the material. Therefore, the samples were subsequently exposed to a thermal treatment (annealing) under isothermal conditions in air. Similarly to experiments on thermal melting, the temperature range to which a superconductor can be heated is very narrow, only 5 – 10 °C. If the maximum temperature is exceeded, the process of laser ablation of the material is initiated and the superconducting properties are irreversibly lost.

The results of studying the surface microstructure of Bi(2223) ceramic samples with the SEM are shown in Fig. 3. An appreciable compaction of the surface is observed in the zone irradiated with the laser beam (Fig. 3a). A transition zone with sharply pronounced dendrites and a pore-free zone, which occupies a width of ~ 1.0 – 1.5 mm, are clearly seen on the side of nonmelted ceramic region. An appropriate selection of laser-melting regimes allows the

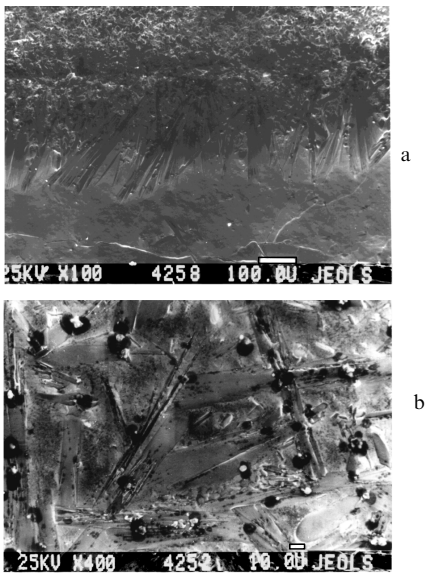

Figure 3. The surface microstructure of a laser-processed Bi(2223) sample: (a) an undoped sample, the boundary layer between the laser-melted region and the nonmelted zone (the scale is 100 μm per division); and (b) a ZrO_2-doped sample (the mass fraction is 2 %) (10 μm per division).

obtainment of rather long equally wide melted grooves with a dense amorphised layer. Specified structures (circuits, rings, etc.) can be obtained with a laser beam scanned according to a preset program.

When Al_2O_3 and ZrO_2 dopants are introduced into the initial Bi(2223) phase, the structure of the resulting surface after the laser irradiation undergoes certain changes (Fig. 3b). The transition zone becomes wider, and the size of the dendrites contained in it increases. Moreover, some groups of inclusions of additional phases in the amorphised zone become noticeable. As the mass fraction of ZrO_2 increases to 5 %, the number of precipitations also increases. Their size is ~ 1 – 2 μm.

After the structure is recrystallised by annealing at $T = 840\,^{\circ}C$ for 4 h, a process of precipitation of crystallites begins (Fig. 4). For comparison, Fig. 5 shows a microphotograph of the initial ceramics with a typical grain size of 5 – 10 μm. The structure acquires a plate-shaped structure (Fig. 4a) in undoped Bi(2223) samples produced by the oxalate method. However, the structure of the samples synthesised at the NPO Monokristall – Reaktiv is essentially different: the grains are smaller and shaped in the form of extended lenses with a cross size of ~ 1.0 – 1.5 μm, and the structure as a whole is denser (Fig. 4b).

In contrast to undoped samples, the recrystallisation process of the amorphised zone of samples doped with Al_2O_3 requires a longer time. During the four first hours of annealing, the amorphised zone preserves a highly dense structure and only initial indications of the formation of crystal grains can be observed. In ZrO_2-doped samples, the recrystallisation process is almost independent of the concentration of the introduced additives.

Hence, the investigations performed show that, due to the laser-induced amorphisation and introduction of various dopants (Al_2O_3, etc.), different types of structures, including those with a stable fine-grained and virtually single-phase

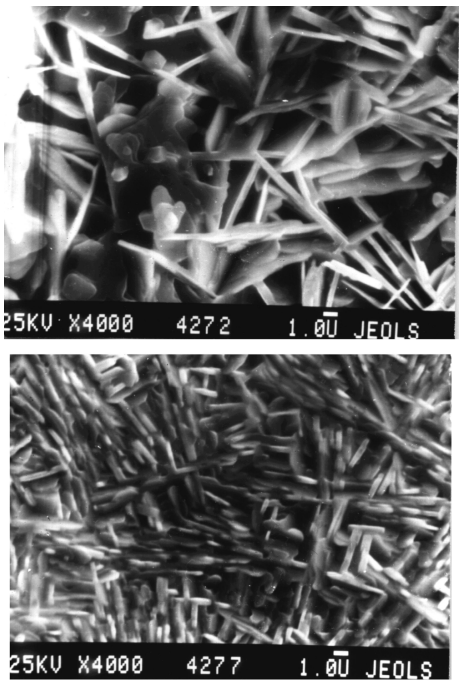

Figure 4. The microstructure of the surface of undoped Bi(2223) samples after laser melting and thermal treatment for 4 h: (a) a sample synthesised at the GIREDMET by the oxalate method and (b) a sample synthesised at the NPO Monokristall – Reaktiv by the ceramic method (the scale is1 μm per division).

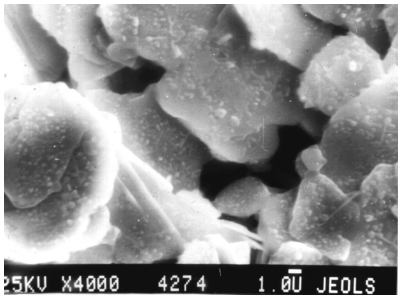

Figure 5. The surface microstructure of the initial undoped sample synthesised at the GIREDMET (the scale is 1 μm per division).

composition, can be formed in Bi-containing HTSC compounds.

Conducting an additional annealing for 10 h results in a further modification of the sample structure. As the annealing duration increases, larger crystallites form in both undoped and ZrO_2-doped samples produced by the oxalate method. In this case, the previously dense amorphised ceramic zone loosens and swells, which is an undesirable process.

There is a difference in the structures of the undoped and doped (the mass fraction of Al_2O_3 is 2 %) samples produced by the ceramic method and exposed to the same thermal treatment. A structure with grains that are ~ 10 times smaller than the grains in the undoped initial sample forms in the doped sample. The latter has a denser structure, and firmly joined grains and their preferential orientation (texture) in local regions can be observed. A texture was not found in samples synthesised by the oxalate method.

The evolution of the phase composition of HTSC ceramic samples at all stages of the sample processing was studied by the X-ray spectrum analysis (using the LINK EDX spectrometer). Fig. 6a shows the data on the elemental content (atomic concentration) of Bi, Sr, Ca, Cu, and Pb at the surface of a Bi(2223) sample. Comparing the contents of elements in the initial sample, after the laser melting and amorphisation, and after the recrystallising thermal treatment shows that, at the first stage, the phase composition corresponds to the ratio of 2 : 2 : 2 : 3, but, after the laser melting and amorphisation, this ratio is modified: the concentrations of Bi and Sr remain almost equal to those in the initial compound (22 % – 24 %), the concentration of Cu increases by ~ 5 %, and the concentration of Ca decreases by 5 % – 7 %. After the annealing at $T = 840\,^{\circ}C$ for 14 h, the chemical composition of the amorphised melted zone begins to recover and approaches the initial composition, implying that the ceramics recrystallises. Introducing Al_2O_3 and ZrO_2 dopants has an insignificant effect on the ratio of elements in the surface layers of nonmelted and melted samples. In both cases, the annealing of the amorphised zone promotes the recovery of the initial chemical composition.

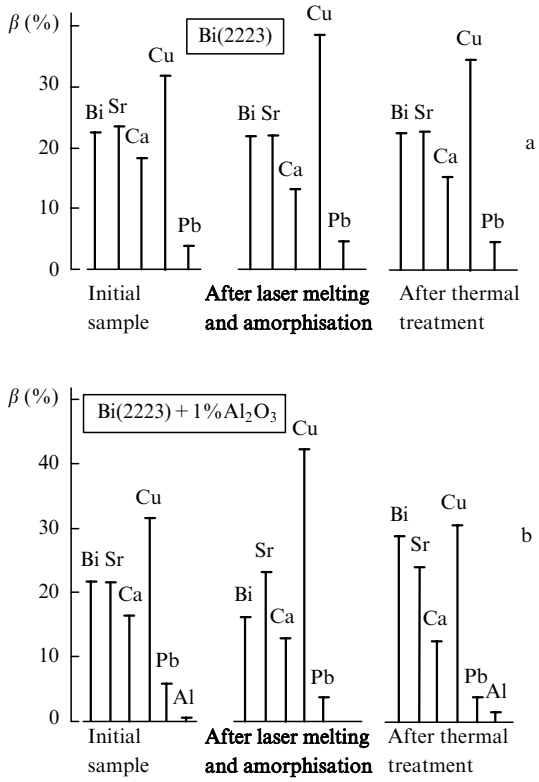

Figure 6. The elemental composition measured using the LINK microanalyser at different stages of laser processing and thermal treatment for (a) Bi(2223) sample and (b) Bi(2223) sample doped with Al_2O_3 (the mass fraction is 1 %).

Fig. 6b shows similar data for a Bi(2223) sample doped with Al_2O_3 (the mass fraction is 1 %). As we see, the phase composition of the initial material completely recovers after a thermal annealing.

An increase in the duration of the laser action up to 20 – 30 s (for rings 2 mm thick with outer and inner diameters of 7 and 3 mm) leads to a complete and irreversible decom-

position of the initial Bi(2223) phase. Microstructure studies have revealed a phase with an increased content of Bi (37.63 % Bi, 25.43 % Sr, 8.627 % Ca, 20.53 % Cu, 6.8 % Pb, and 0.9 % Al). In its turn, the basic matrix is significantly depleted of Bi (1.8 % Bi, 17.829 % Sr, 16.26 % Ca, 0.113 % Pb, and 0.921 % Al).

Laser melting of the $YBa_2Cu_3O_{7-x}$ and $(BiPb)_2Sr_2Ca_2Cu_3O_{10-y}$ superconducting ceramics was also investigated. The radiation power density of the CO_2 laser could be varied within a wide range up to 127 W cm^{-2} by focusing the beam. The sample surface was scanned once or twice at a speed of 45 mm min^{-1}. After laser melting, YBCO(123) and Bi(2223) samples were annealed under isothermal conditions at 920 °C for 50 h and 840 °C for 100 h, respectively.

The results of experiments show an essential difference in the changes in YBCO(123) and Bi(2223) HTSC ceramic microstructures. Laser melting and annealing insignificantly modify the YBCO(123) microstructure, but the Bi(2223) microstructure changes significantly. As a result of laser melting and annealing, a flat structure with local (40×50 μm) textured zones appears in it.

The results of the offered laser-melting technique combined with a short-duration thermal annealing have found an obvious representation in experiments on measurements of the critical current density j_c. Fig. 7 shows the temperature dependences of j_c for Bi(2223) samples for various laser-irradiation regimes. One can see that for the optimal processing conditions, j_c at $T = 20$ and 77 K increases by a factor of 40 and 8, respectively, compared to the initial sample. In both cases, T_c remains constant.

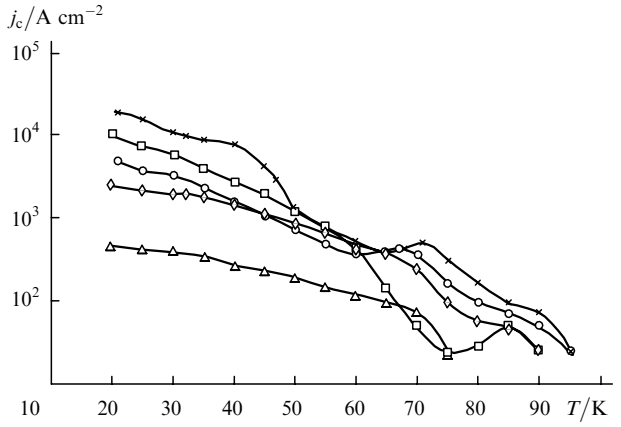

Figure 7. Temperature dependences of the critical current density before and after laser melting and annealing: (△) the initial Bi(2223) ceramics prepared by the compaction method; (○) a sample melted by 10.6-μm CO_2 laser radiation with a power density $q = 57$ W cm^{-2}, the sample surface is singly scanned at a speed of 45 mm min^{-1}; $q = 44$ W cm^{-2}, the sample surface is scanned (□) twice and (◇) once at a speed of 45 mm min^{-1}; and (×) $q = 127$ W cm^{-2}, the sample surface is scanned once at a speed of 45 mm min^{-1}. After laser melting, the samples were annealed under isothermal conditions at 840 °C for 100 h.

Note that these data of j_c measurements refer to the entire sample with a thickness of ~ 1 mm but not only to the surface layer, as was in Refs [12–14], where 1.06-μm pulsed radiation was used.

No significant increase in j_c was observed after laser melting and subsequent annealing of yttrium-based YBCO(123) ceramic samples. A reasonable explanation for this effect is that the YBCO(123) ceramics must be annealed in oxygen but not in air.

The results of the XRD analysis of Bi(2223) samples show that the initial material consisted of the Bi(2223) phase (67 %), Bi(2212) phase (23 %), and other impurities (10 %). As a result of laser melting, the Bi(2223) phase decays and the Bi(2201) phase forms. The subsequent annealing leads to the formation of the Bi(2212) phase (in 50 h) and then to the recovery of the Bi(2223) phase (> 60 % in 100 h). These results are confirmed by measurements of the magnetic susceptibility χ (Fig. 8). The curves $\chi(T)$ have three steps at $T > 115$, 100, and 70 K, which may arise as a result of superconducting transitions in the bulk and at the boundaries of the Bi(2223) and Bi(2212) phase grains, respectively.

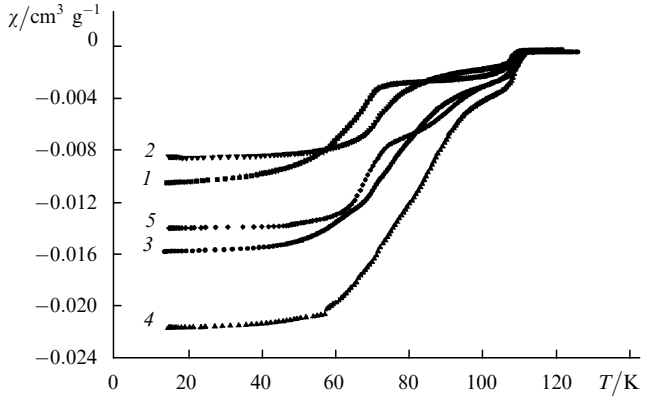

Figure 8. Temperature dependences of the magnetic susceptibility before and after laser melting and thermal annealing: (*1*) the initial Bi(2223) ceramics prepared by the compaction method; (*2*) a sample melted by 10.6-μm CO_2 laser radiation with a power density $q = 57$ W cm^{-2}, the sample surface is scanned once at a speed of 45 mm min^{-1}; $q = 44$ W cm^{-2} the sample surface is scanned (*3*) once and (*4*) twice at a speed of 45 mm min^{-1}; and (*5*) $q = 127$ W cm^{-2}, the sample surface is scanned once at a speed of 45 mm min^{-1}. After laser melting, the samples were annealed under isothermal conditions at 840 °C for 100 h.

5. Conclusions

The presented data testify to a high efficiency of applying lasers to the improvement of current-carrying properties of HTSC ceramic samples. By varying the radiation wavelength and lasing modes (cw or pulsed), the recrystallisation depth can be varied from a few micrometers to millimetres, depending on a particular problem.

Investigations of the microstructure and chemical composition of samples and the superconducting parameters demonstrate that, using the techniques of laser melting of HTSC ceramics combined with a short-duration thermal annealing, it is possible to substantially increase the critical-current density up to $j_c = 10^4 - 10^5$ A cm^{-2}. In some cases, annealing is unnecessary. An increase in j_c is caused mainly by a compaction of the ceramics and an improvement of the contacts between grains. A textured structure can be formed.

In further investigations, it is scheduled to improve the described laser techniques.

Acknowledgements. We are grateful to the co-authors of the cited papers.

References

1. Golovashkin A.I., Ekimov E.V., Krasnosvobodtsev S.I., Pechen E.V. *Physica C*, **153–155**, 1455 (1988).
2. Gridnev V.N., Dekhter I.Ya.,Ivanov L.I., Karlov N.V., Kuz'min G.P., Nishchenko M.M., Prokhorov A.M., Rykalin N.N., Yanushkevich V.A. *Pis'ma Zh. Eksp. Teor. Fiz.*, **18** (4), 258 (1973).
3. Mikhailichenko A.L., Mikhailova G.N., Prokhorov A.M., Seferov A.S., Troitskii A.V., Mednikov A.O., Mikhailov B.P., Burkhanov G.S., Lapshina I.E. *Kvantovaya Elektron.*, **23**, 715 (1996) [*Quantum Electron.*, **26**, 696 (1996)].
4. Mikhailova G.N., Prokhorov A.M., Troitskii A.V., Mikhailov B.P., Grigorashev D.I., Kazin P.E., Lennikov V.V., Aksenova T.D. *Proc. SPIE Int. Soc. Opt. Eng.*, **3404**, 230 (1997).
5. Mikhailova G.N., Prokhorov A.M., Troitskii A.V., Mikhailov B.P., Grigorashev D.I., Kazin P.E., Lennikov V.V., Aksenova T.D. *Kratk. Soobshch. Fiz. FIAN*, (10), 25 (1999).
6. Jagannadham K., Narayan J. *Mater. Sci. Eng. B*, **8**, 201 (1991).
7. Ekin J.W., Braginski A.I., Panson A.J., et al. *J. Appl. Phys.*, **62** (12), 4821 (1987).
8. Li S.R., Oleinikov N.N., Gudilin E.A. *Neorg. Mater.*, **29** (1), 3 (1993).
9. Jin S., Tiefil T.H., Sherwood R.C., et al. *Phys. Rev. B*, **37** (13), 7850 (1988).
10. Cava J.R., Batlogg B., van Dover R.B., et al. *Phys. Rev. Lett.*, **58** (16), 1676 (1987).
11. Kupfer H., Keller C., Meier-Hirmer R., et al. *IEEE Trans. Magn.*, **27** (2), 1369 (1991).
12. Gorol'chuk I.G., Ul'yashin A.G., Bumai Yu.A., Esepkin V.A., Domanevskii D.S., Malakhovskaya V.E., Bliznyuk N.V., Tatur G.A., Batishche S.A., Kuz'muk A.A. *Sverkhprovodimost: Fiz., Khim., Tekh.*, **3** (11), 2616 (1990).
13. Esepkin V.A., Ul'yashin A.G., Gorol'chuk I.G., Bliznyuk N.V., Bumai Yu.A., Tatur G.A., Batishche S.A., Kuz'muk A.A., Kononyuk N.F., Makhnach A.V., Lomonosov V.A. *Sverkhprovodimost: Fiz., Khim., Tekh.*, **4** (7), 1344 (1991).
14. Denisov Yu.V., Madii V.A., Krasilov Yu.I. *Sverkhprovodimost: Fiz., Khim., Tekh.*, **7** (1), 109 (1994).
15. El Azrak A., Nahoum R., Bontemps N., et al. *Phys. Rev. B*, **49** (14), 9846 (1994).
16. Mikhailov B.P., Burkhanov G.S., Leitus G.M., Mikhailova G.N., Prokhorov A.M., Seferov A.S., Troitskii A.V., Lapshina I.E. *Neorg. Mater.*, **32** (10), 1225 (1996).

Session of the General Physics and Astronomy Department, Academy of Sciences of the USSR, in Tashkent, in the late 1980s.